nature climate change

Supplementary information

https://doi.org/10.1038/s41558-024-02031-0

# Novel temperatures are already widespread beneath the world's tropical forest canopies

In the format provided by the authors and unedited

## Table of Contents

Supplementary Tables

**Table S1-1: Mean and standard deviation values of novelty in temperature regimes across Africa.** Forest is classed as either undisturbed tropical forest where wilderness areas are excluded (n = 59,001), undisturbed tropical forest in wilderness areas only (n = 8,798), or degraded tropical forest only (n = 12,800).

| | Undisturbed - Wilderness | | Undisturbed | | Degraded | |
|---|---|---|---|---|---|---|
| **Variable** | **Mean** | **S.D.** | **Mean** | **S.D.** | **Mean** | **S.D.** |
| BIO 1 | 0.61 | 0.09 | 0.60 | 0.12 | 0.57 | 0.14 |
| BIO 2 | 0.51 | 0.16 | 0.51 | 0.17 | 0.48 | 0.17 |
| BIO 3 | 0.27 | 0.10 | 0.28 | 0.12 | 0.25 | 0.17 |
| BIO 4 | 0.38 | 0.19 | 0.40 | 0.18 | 0.38 | 0.16 |
| BIO 5 | 0.37 | 0.12 | 0.38 | 0.13 | 0.38 | 0.14 |
| BIO 6 | 0.32 | 0.11 | 0.28 | 0.10 | 0.29 | 0.11 |
| BIO 7 | 0.28 | 0.10 | 0.30 | 0.12 | 0.31 | 0.12 |

**Table S1-2: Mean and standard deviation values of novelty in temperature regimes across Central and South America.** Forest is classed as either undisturbed tropical forest where wilderness areas are excluded (n = 98,612), undisturbed tropical forest in wilderness areas only (n = 87,271), or degraded tropical forest only (n = 22,119).

| | Undisturbed - Wilderness | | Undisturbed | | Degraded | |
|---|---|---|---|---|---|---|
| **Variable** | **Mean** | **S.D.** | **Mean** | **S.D.** | **Mean** | **S.D.** |
| BIO 1 | 0.51 | 0.14 | 0.52 | 0.16 | 0.50 | 0.19 |
| BIO 2 | 0.54 | 0.19 | 0.50 | 0.19 | 0.42 | 0.18 |
| BIO 3 | 0.27 | 0.12 | 0.26 | 0.10 | 0.26 | 0.10 |
| BIO 4 | 0.44 | 0.17 | 0.40 | 0.16 | 0.35 | 0.16 |
| BIO 5 | 0.37 | 0.12 | 0.38 | 0.13 | 0.38 | 0.14 |
| BIO 6 | 0.32 | 0.11 | 0.28 | 0.10 | 0.29 | 0.11 |
| BIO 7 | 0.28 | 0.10 | 0.30 | 0.12 | 0.31 | 0.12 |

**Table S1-3: Mean and standard deviation values of novelty in temperature regimes across Asia & Australia.** Forest is classed as either undisturbed tropical forest where wilderness areas are excluded (n = 50,127), undisturbed tropical forest in wilderness areas only (n = 14,000), and degraded tropical forest only (n = 21,469).

| | Undisturbed - Wilderness | | Undisturbed | | Degraded | |
|---|---|---|---|---|---|---|
| **Variable** | **Mean** | **S.D.** | **Mean** | **S.D.** | **Mean** | **S.D.** |
| BIO 1 | 0.56 | 0.13 | 0.48 | 0.14 | 0.47 | 0.13 |
| BIO 2 | 0.30 | 0.12 | 0.33 | 0.14 | 0.32 | 0.15 |
| BIO 3 | 0.24 | 0.10 | 0.27 | 0.11 | 0.28 | 0.10 |
| BIO 4 | 0.32 | 0.12 | 0.33 | 0.13 | 0.31 | 0.14 |
| BIO 5 | 0.39 | 0.15 | 0.33 | 0.12 | 0.31 | 0.12 |
| BIO 6 | 0.36 | 0.13 | 0.33 | 0.13 | 0.32 | 0.13 |
| BIO 7 | 0.26 | 0.10 | 0.28 | 0.11 | 0.27 | 0.11 |

**Table S2-1: Results of piecewise generalised linear models (GLMs) for Central and South America.** For each temperature variable (*n* = *7*), GLMs with a binomial logit were fit to the relationship between the below-canopy novelty of a variable and the change in the same variable (i.e. the difference between the mean of 1990 - 2004 and the mean of 2005 - 2019) across undisturbed tropical forests in Central and South America (*n* = *185,883*). Tests were conducted using two-sided Wald tests with a significance level set at $p < 0.01$. Each temperature variable was analysed and presented separately, so no adjustments were made for multiple comparisons.

| Variable | Direction of mean change | Estimate | Std.error | p.value | 2.5% CI | 97.5% CI | Deviance |
|---|---|---|---|---|---|---|---|
| BIO 1 | positive | -2.33 | 0.517 | 6.669E-06 | -3.34 | -1.31 | 40.71 |
| BIO 1 | negative | 3.51 | 0.033 | 0.000E+00 | 3.45 | 3.58 | 5145.83 |
| BIO 2 | positive | -2.51 | 0.085 | 2.387E-191 | -2.68 | -2.35 | 915.14 |
| BIO 2 | negative | 2.77 | 0.025 | 0.000E+00 | 2.73 | 2.82 | 8544.23 |
| BIO 3 | positive | -38.21 | 0.880 | 0.000E+00 | -39.94 | -36.49 | 3017.49 |
| BIO 3 | negative | 32.96 | 0.661 | 0.000E+00 | 31.67 | 34.26 | 2769.82 |
| BIO 4 | positive | -0.94 | 0.032 | 1.537E-185 | -1.00 | -0.88 | 2029.66 |
| BIO 4 | negative | 1.80 | 0.018 | 0.000E+00 | 1.76 | 1.83 | 6544.07 |
| BIO 5 | positive | -0.72 | 0.058 | 7.544E-36 | -0.83 | -0.61 | 431.46 |
| BIO 5 | negative | 1.04 | 0.009 | 0.000E+00 | 1.02 | 1.06 | 8489.92 |
| BIO 6 | positive | -0.91 | 0.052 | 5.254E-68 | -1.02 | -0.81 | 1147.87 |
| BIO 6 | negative | 0.60 | 0.021 | 3.289E-177 | 0.56 | 0.64 | 7852.20 |
| BIO 7 | positive | -0.61 | 0.041 | 1.107E-49 | -0.69 | -0.53 | 758.40 |
| BIO 7 | negative | 0.69 | 0.010 | 0.000E+00 | 0.67 | 0.71 | 7050.58 |

**Table S2-2: Results of piecewise generalised linear models (GLMs) for Africa.** For each temperature variable (*n = 7*), GLMs with a binomial logit were fit to the relationship between the below-canopy novelty of a variable and the change in the same variable (i.e. the difference between the mean of 1990 - 2004 and the mean of 2005 - 2019) across undisturbed tropical forests in Africa (*n = 67,799*). Tests were conducted using two-sided Wald tests with a significance level set at $p < 0.01$. Each temperature variable was analysed and presented separately, so no adjustments were made for multiple comparisons.

| Variable | Direction of mean change | Estimate | Std.error | p.value | 2.5% CI | 97.5% CI | Deviance |
|---|---|---|---|---|---|---|---|
| BIO 1 | positive | -1.48 | 0.728 | 4.142E-02 | -2.93 | -0.05 | 18.89 |
| BIO 1 | negative | 2.72 | 0.060 | 0.000E+00 | 2.61 | 2.84 | 1535.22 |
| BIO 2 | positive | -1.50 | 0.121 | 1.813E-35 | -1.74 | -1.27 | 362.12 |
| BIO 2 | negative | 2.72 | 0.053 | 0.000E+00 | 2.62 | 2.83 | 2874.88 |
| BIO 3 | positive | -34.35 | 1.609 | 3.772E-101 | -37.52 | -31.21 | 839.89 |
| BIO 3 | negative | 39.40 | 1.055 | 5.589E-305 | 37.33 | 41.47 | 1415.03 |
| BIO 4 | positive | -1.19 | 0.051 | 6.532E-119 | -1.29 | -1.09 | 545.71 |
| BIO 4 | negative | 2.74 | 0.043 | 0.000E+00 | 2.66 | 2.82 | 2582.87 |
| BIO 5 | positive | -0.56 | 0.063 | 5.948E-19 | -0.69 | -0.44 | 169.84 |
| BIO 5 | negative | 0.92 | 0.024 | 0.000E+00 | 0.88 | 0.97 | 2355.72 |
| BIO 6 | positive | -0.70 | 0.072 | 2.969E-22 | -0.84 | -0.56 | 1061.80 |
| BIO 6 | negative | 0.74 | 0.023 | 1.522E-235 | 0.70 | 0.78 | 1732.37 |
| BIO 7 | positive | -0.61 | 0.032 | 1.882E-83 | -0.67 | -0.55 | 335.59 |
| BIO 7 | negative | 0.84 | 0.025 | 3.174E-247 | 0.79 | 0.88 | 2090.32 |

**Table S2-3: Results of piecewise generalised linear models (GLMs) for** Asia and Australia**.** For each temperature variable (*n = 7*), GLMs with a binomial logit were fit to the relationship between the below-canopy novelty of a variable and the change in the same variable (i.e. the difference between the mean of 1990 - 2004 and the mean of 2005 - 2019) across undisturbed tropical forests in Asia and Australia (*n = 64,127*). Tests were conducted using two-sided Wald tests with a significance level set at $p < 0.01$. Each temperature variable was analysed and presented separately, so no adjustments were made for multiple comparisons.

| Variable | Direction of mean change | Estimate | Std.error | p.value | 2.5% CI | 97.5% CI | Deviance |
|---|---|---|---|---|---|---|---|
| BIO 1 | positive | -1.77 | 0.332 | 1.021E-07 | -2.43 | -1.13 | 56.27 |
| BIO 1 | negative | 2.70 | 0.057 | 0.000E+00 | 2.59 | 2.81 | 2274.81 |
| BIO 2 | positive | -1.75 | 0.057 | 5.787E-204 | -1.86 | -1.64 | 1668.68 |
| BIO 2 | negative | 2.13 | 0.063 | 3.427E-248 | 2.01 | 2.26 | 1003.71 |
| BIO 3 | positive | -35.91 | 1.747 | 6.307E-94 | -39.33 | -32.48 | 795.98 |
| BIO 3 | negative | 31.66 | 1.179 | 6.326E-159 | 29.35 | 33.97 | 1166.13 |
| BIO 4 | positive | 0.00 | 0.000 | 2.735E-01 | 0.00 | 0.00 | 3275.63 |
| BIO 4 | negative | 0.00 | 0.000 | 4.123E-02 | 0.00 | 0.00 | 618.53 |
| BIO 5 | positive | -0.31 | 0.022 | 1.948E-44 | -0.35 | -0.26 | 665.50 |
| BIO 5 | negative | 0.53 | 0.026 | 2.803E-90 | 0.48 | 0.58 | 3005.13 |
| BIO 6 | positive | -0.52 | 0.109 | 2.112E-06 | -0.73 | -0.30 | 170.61 |
| BIO 6 | negative | 0.90 | 0.026 | 1.651E-258 | 0.85 | 0.96 | 2556.01 |
| BIO 7 | positive | -0.40 | 0.016 | 7.339E-141 | -0.43 | -0.37 | 1494.07 |
| BIO 7 | negative | 0.30 | 0.030 | 2.734E-23 | 0.24 | 0.36 | 831.55 |

**Table S3: Summary of temperature loggers used to validate the microclimate model.**

| Continental Area | Countries | No. of loggers | Years | Total duration (days) | Mean Duration (days) | Elevation range (m) |
|---|---|---|---|---|---|---|
| South America | Peru | 6 | 2014, 2015, 2019 | 1146 | 191 | 2842 |
| | Ecuador | 1 | 2006 | 365 | 365 | 0 |
| | Brazil | 9 | 2019, 2020, 2023 | 1952 | 217 | 34 |
| Africa | DRC | 3 | 2016, 2017 | 611 | 204 | 1570 |
| | Uganda | 7 | 2018 | 1797 | 257 | 1622 |
| | Kenya | 5 | 2020 | 1830 | 366 | 1740 |
| Southeast Asia | Malaysia | 39 | 2015, 2016, 2019 | 5871 | 151 | 443 |

**Table S4: Summary of changes in temperature variables.** Shown as number of years in the recent period (2005 to 2019) where temperature variables were greater than the maximum of all years in the historic baseline period (1990 to 2004).

| Temperature Variable | Number of years | Greatest increase (ºC) | Continental Group |
|---|---|---|---|
| BIO 1 | 6 | 0.4 | Africa |
| BIO 1 | 4 | 0.25 | Central & South America |
| BIO 1 | 0 | 0.00 | Southeast Asia & Australia |
| BIO 2 | 11 | 0.30 | Africa |
| BIO 2 | 15 | 0.32 | Central & South America |
| BIO 2 | 0 | 0.00 | Southeast Asia & Australia |
| BIO 4 | 2 | 0.10 | Africa |
| BIO 4 | 8 | 0.32 | Central & South America |
| BIO 4 | 2 | 1.00 | Southeast Asia & Australia |

**Table S5: Breakdown of novelty scores.** The percentage of tropical forest grid cells with low (0 to 0.2) to high (0.81 to 1) recent fractional novelty across all modelled temperature variables; classified by continental group: CSA (Central & South America), AFR (Africa), SEAA (Southeast Asia & Australia).

| Variable | Group | 0-0.2 (%) | 0.21-0.4 (%) | 0.41-0.6 (%) | 0.61-0.8 (%) | 0.81-1.0 (%) |
|---|---|---|---|---|---|---|
| BIO 1 | CSA | 3 | 21 | 49 | 24 | 3 |
| BIO 1 | AFR | 1 | 8 | 35 | 56 | 0 |
| BIO 1 | SEAA | 2 | 26 | 48 | 24 | 0 |
| BIO 2 | CSA | 7 | 28 | 33 | 27 | 4 |
| BIO 2 | AFR | 4 | 28 | 40 | 28 | 0 |
| BIO 2 | SEAA | 23 | 58 | 16 | 3 | 0 |
| BIO3 | CSA | 42 | 50 | 8 | 0 | 0 |
| BIO 3 | AFR | 40 | 51 | 9 | 1 | 0 |
| BIO 3 | SEAA | 41 | 52 | 6 | 0 | 0 |
| BIO 4 | CSA | 13 | 45 | 30 | 12 | 1 |
| BIO 4 | AFR | 17 | 38 | 30 | 15 | 0 |
| BIO 4 | SEAA | 22 | 59 | 18 | 1 | 0 |
| BIO 5 | CSA | 8 | 35 | 33 | 21 | 2 |
| BIO 5 | AFR | 8 | 49 | 40 | 3 | 0 |
| BIO 5 | SEAA | 17 | 57 | 24 | 2 | 0 |
| BIO 6 | CSA | 34 | 56 | 10 | 0 | 0 |
| BIO 6 | AFR | 32 | 57 | 11 | 1 | 0 |
| BIO 6 | SEAA | 18 | 59 | 22 | 1 | 0 |
| BIO 7 | CSA | 28 | 56 | 15 | 1 | 0 |
| BIO 7 | AFR | 22 | 60 | 17 | 1 | 0 |
| BIO 7 | SEAA | 36 | 57 | 7 | 1 | 0 |

**Table S6: Datasets used for microclimate modelling.** Input data products, and the variables extracted from them, used to parameterize the *microclimf* microclimate model specific to validating empirical temperature observations.

| Product | Variable(s) used | Spatial Resolution | Spatial Extent | Temporal Resolution | Temporal Extent | Remarks | Citation |
|---|---|---|---|---|---|---|---|
| ECMWF ERA5 reanalysis | 2m temperature, 2m dewpoint temperature, surface pressure, 10m u wind, 10m v wind, total precipitation, total cloud cover, mean surface net longwave radiation flux, mean surface downward longwave radiation flux, total sky direct solar radiation at surface, surface downward solar radiation | 0.25 decimal degrees | global | hourly | 1950 - present | None | Hersbach et al., 2020 |
| ESA CCI Land Cover | Land cover categories | 300m | global | annual | 1992 - one year from present | Used for predictions in years before 2015 | ESA, 2017 |
| Copernicus Global Land Service Land Cover | Land cover categories | 100m | global | annual | 2015 - two years from present | Used for predictions in years 2015 or later | Buchhorn et al., 2020 |
| Potapov et al. 2020 | Vegetation Canopy Height | 30m | within 52°N and 52°S globally | static | 2019 | Used for latitudes between 52°N and 52°S | Potapov et al., 2020 |
| Simard et al. 2011 | Vegetation Canopy Height | 1000m | global (employed for above 52°N and 52°S) | static | 2005 | Used for latitudes outside of 52°N and 52°S | Simard et al., 2011 |
| MODIS MOD15A2H | LAI (Leaf Area Index) Stage 2 | 500m | global | 8 days | 2000 - 2020 | | Myneni et al., 2015 |
| ISRIC-WISE | Soil bulk density and percent clay, silt, and sand at 0cm, 5cm, 15cm, 30cm, 60cm, and 100cm depths | 0.05 decimal degrees | global | static | spatial data sources from 1970s to 2000s | | Batjes et al., 2016 |
| ASTER Global Digital Elevation Map | Elevation (GDEM V3) | 30m | global | static | Launched in 1999 | | Fujisada et al., 2005 |

Supplementary Figures

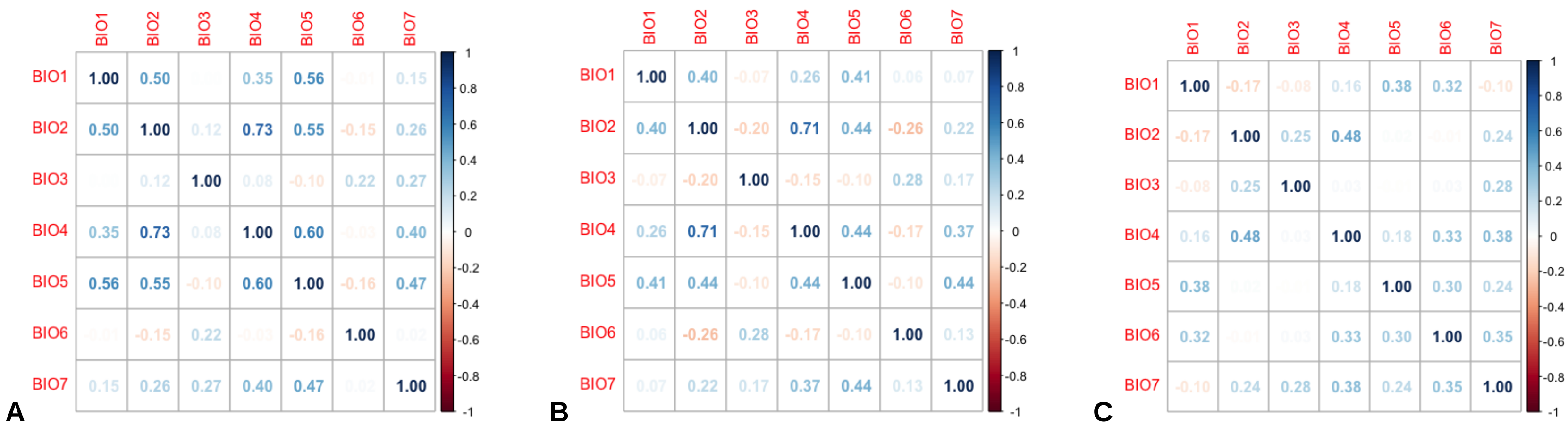

**Fig. S1: Spearman's correlation coefficient for novelty scores of all temperature variables.** Separated by continental group: (a) South and Central America, (b) Africa, and (c) Southeast Asia and Australia.

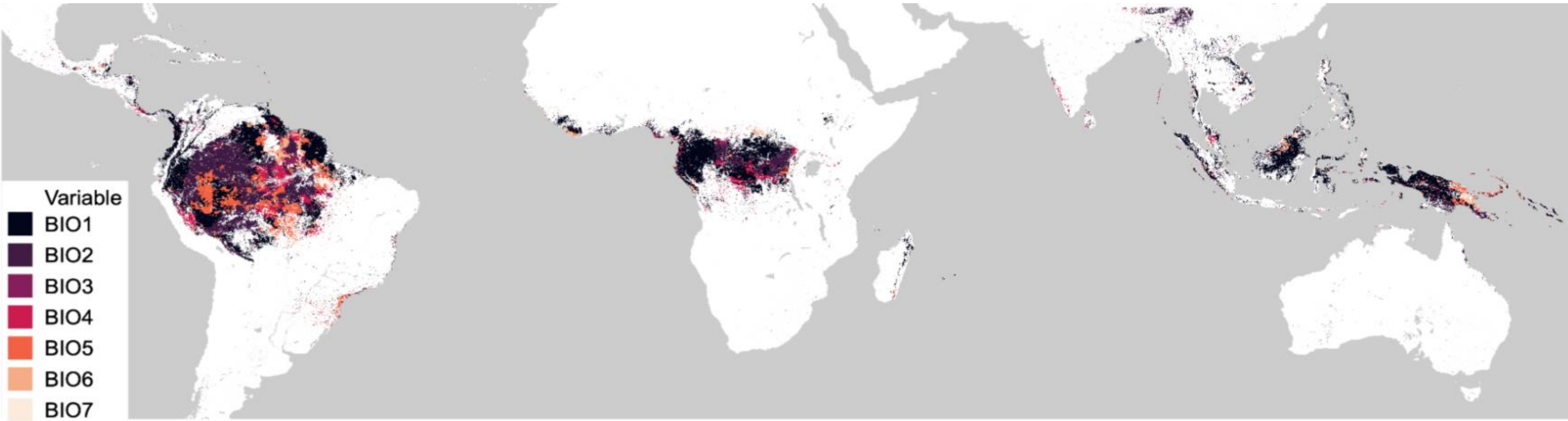


**Fig. S2: Undisturbed tropical forest locations showing which temperature variable had the greatest influence on the index of cumulative novelty in temperature.** Temperature variables (n = 7) include: mean annual temperature (BIO1), mean diurnal temperature range (BIO2), isothermality (BIO3), temperature seasonality (BIO4), maximum temperature of the warmest month (BIO5), minimum temperature of the coldest month (BIO6), annual temperature range (BIO7).


**Fig. S3-1: The difference between the novelty of mean annual temperatures below the canopy and the novelty of mean annual temperatures from the ERA5 reanalysis climate data.** Calculated across global undisturbed tropical forests as the novelty of the below canopy variable minus the novelty of the variable derived from ERA5. Plot, inset right, shows the distribution of the difference in novelty scores for the temperature variable between continental groups (Central & South America, Africa, and Southeast Asia & Australia). A difference value greater than 0 indicates a higher novelty score for the below-canopy version of the variable.

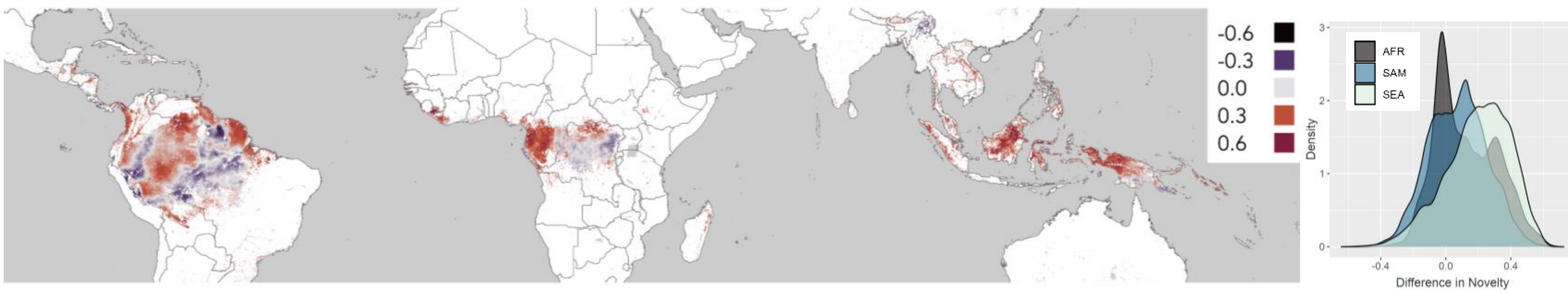


**Fig. S3-2: The difference between the novelty of the mean diurnal temperature range below the canopy and the novelty of the mean diurnal temperature range from the ERA5 reanalysis climate data.** Calculated across global undisturbed tropical forests as the novelty of the below canopy variable minus the novelty of the variable derived from ERA5. Plot, inset right, shows the distribution of the difference in novelty scores for the temperature variable between continental groups (Central & South America, Africa, and Southeast Asia & Australia). A difference value greater than 0 indicates a higher novelty score for the below-canopy version of the variable.

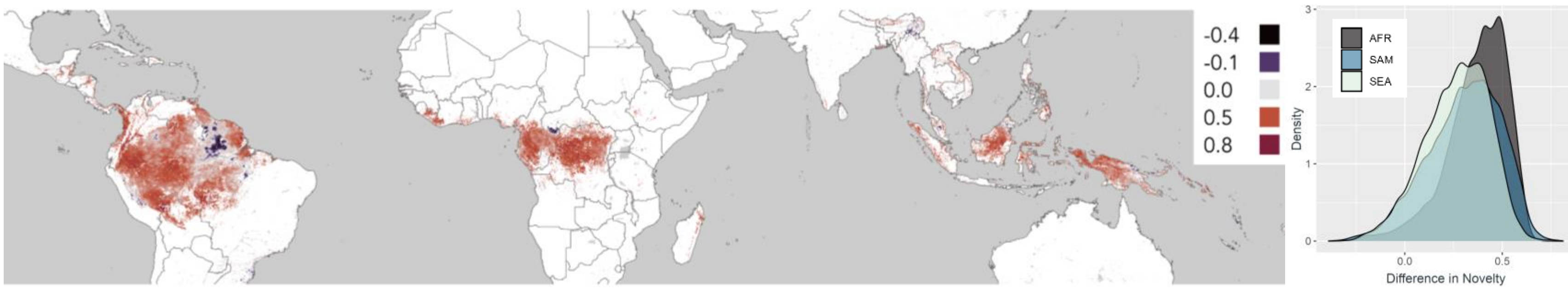


**Fig. S3-3: The difference between the novelty of isothermality below the canopy and the novelty of isothermality from the ERA5 reanalysis climate data.** Calculated across global undisturbed tropical forests as the novelty of the below canopy variable minus the novelty of the variable derived from ERA5. Plot, inset right, shows the distribution of the difference in novelty scores for the temperature variable between continental groups (Central & South America, Africa, and Southeast Asia & Australia). A difference value greater than 0 indicates a higher novelty score for the below-canopy version of the variable.

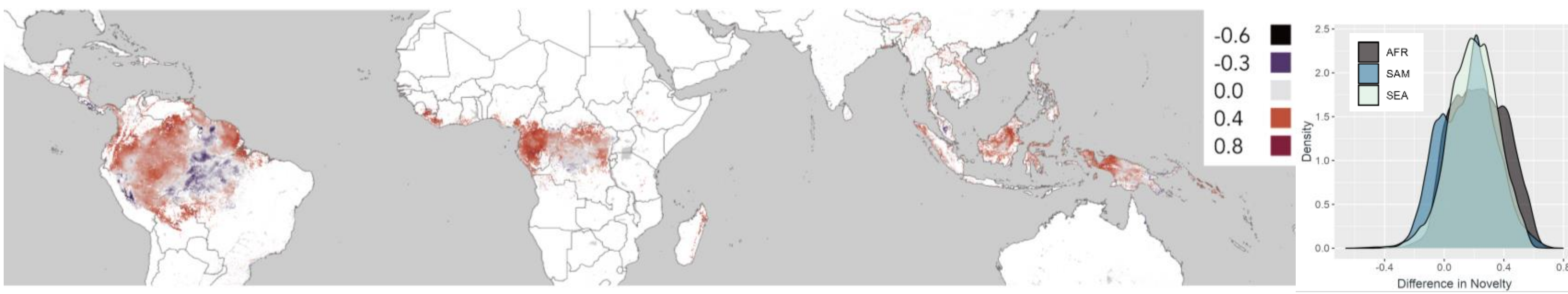


**Fig. S3-4: The difference between the novelty of temperature seasonality below the canopy and the novelty of temperature seasonality from the ERA5 reanalysis climate data.** Calculated across global undisturbed tropical forests as the novelty of the below canopy variable minus the novelty of the variable derived from ERA5. Plot, inset right, shows the distribution of the difference in novelty scores for the temperature variable between continental groups (Central & South America, Africa, and Southeast Asia & Australia). A difference value greater than 0 indicates a higher novelty score for the below-canopy version of the variable.


**Fig. S3-5: The difference between the novelty of the maximum temperature of the warmest month below the canopy and the novelty of the maximum temperature of the warmest month from the ERA5 reanalysis climate data.** Calculated across global undisturbed tropical forests as the novelty of the below canopy variable minus the novelty of the variable derived from ERA5. Plot, inset right, shows the distribution of the difference in novelty scores for the temperature variable between continental groups (Central & South America, Africa, and Southeast Asia & Australia). A difference value greater than 0 indicates a higher novelty score for the below-canopy version of the variable.

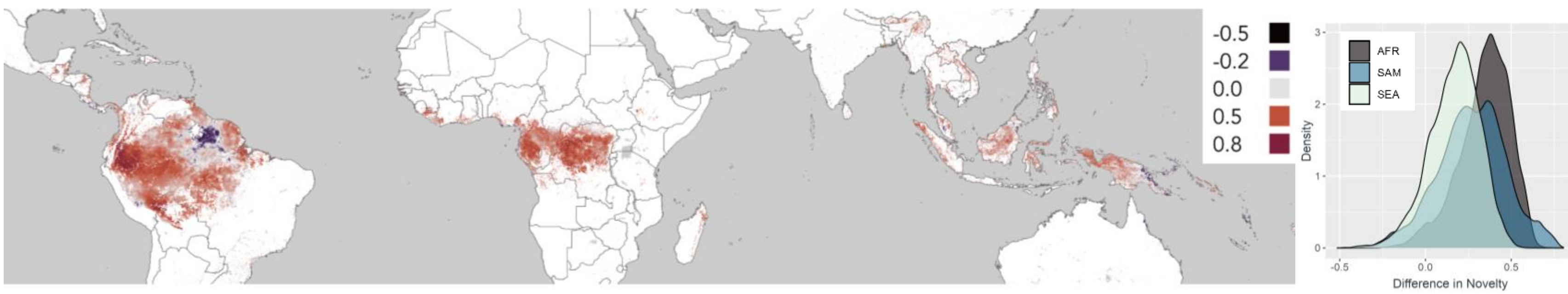


**Fig. S3-6: The difference between the novelty of the minimum temperature of the coldest month below the canopy and the novelty of the minimum temperature of the coldest month from the ERA5 reanalysis climate data.** Calculated across global undisturbed tropical forests as the novelty of the below canopy variable minus the novelty of the variable derived from ERA5. Plot, inset right, shows the distribution of the difference in novelty scores for the temperature variable between continental groups (Central & South America, Africa, and Southeast Asia & Australia). A difference value greater than 0 indicates a higher novelty score for the below-canopy version of the variable.

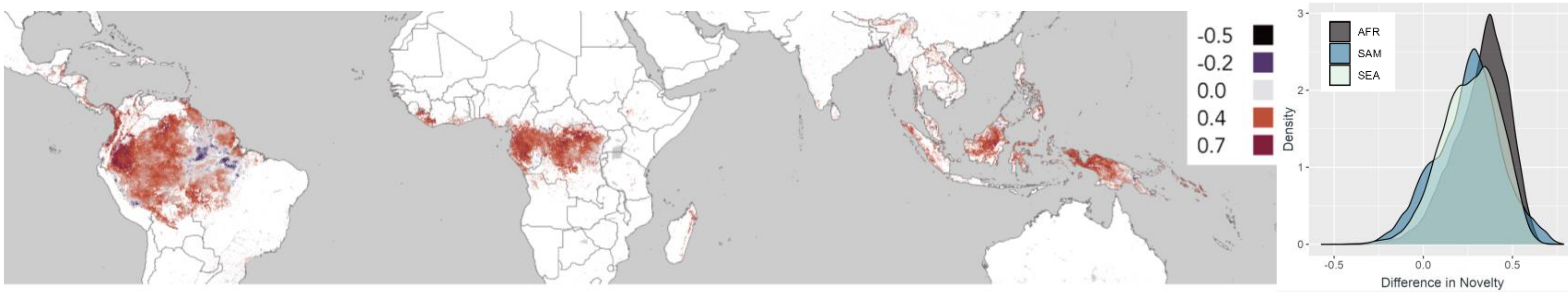


**Fig. S3-7: The difference between the novelty of the annual temperature range below the canopy and the novelty of the annual temperature range from the ERA5 reanalysis climate data.** Calculated across global undisturbed tropical forests as the novelty of the below canopy variable minus the novelty of the variable derived from ERA5. Plot, inset right, shows the distribution of the difference in novelty scores for the temperature variable between continental groups (Central & South America, Africa, and Southeast Asia & Australia). A difference value greater than 0 indicates a higher novelty score for the below-canopy version of the variable.

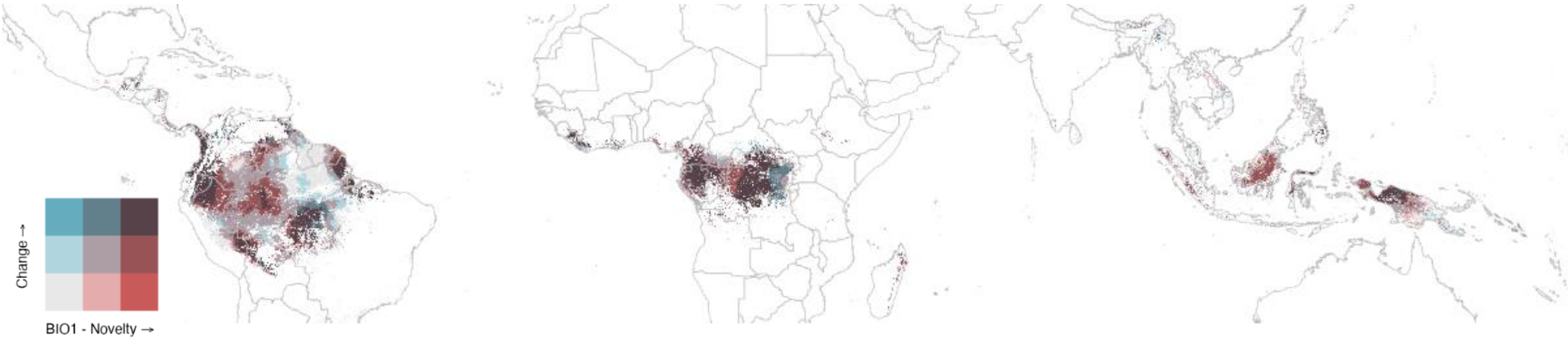


**Fig. S4-1: Spatial relationship between the overall change (°C) and the recent novelty of mean annual temperature.** Change is defined as the difference between the mean of the temperature variable for 1990-2004 and the mean for 2005-2019.

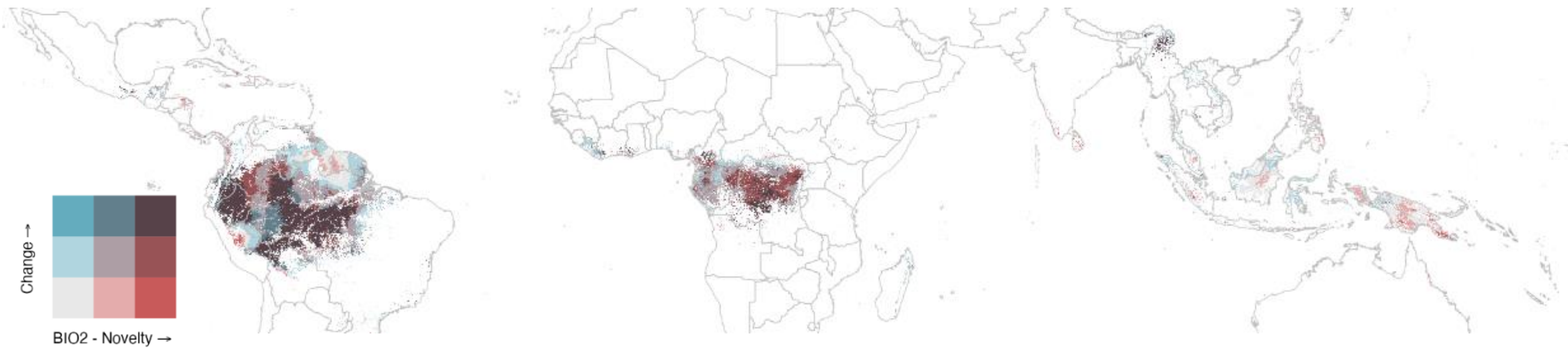


**Fig. S4-2: Spatial relationship between the overall change (°C) and the recent novelty of mean diurnal temperature range.** Change is defined as the difference between the mean of the temperature variable for 1990-2004 and the mean for 2005-2019.

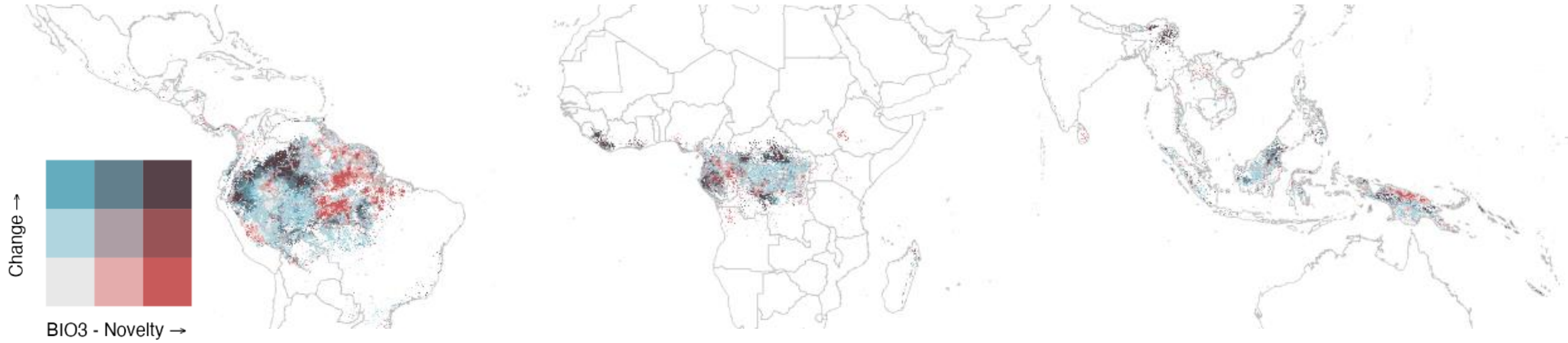


**Fig. S4-3: Spatial relationship between the overall change (°C) and the recent novelty of isothermality.** Change is defined as the difference between the mean of the temperature variable for 1990-2004 and the mean for 2005-2019.

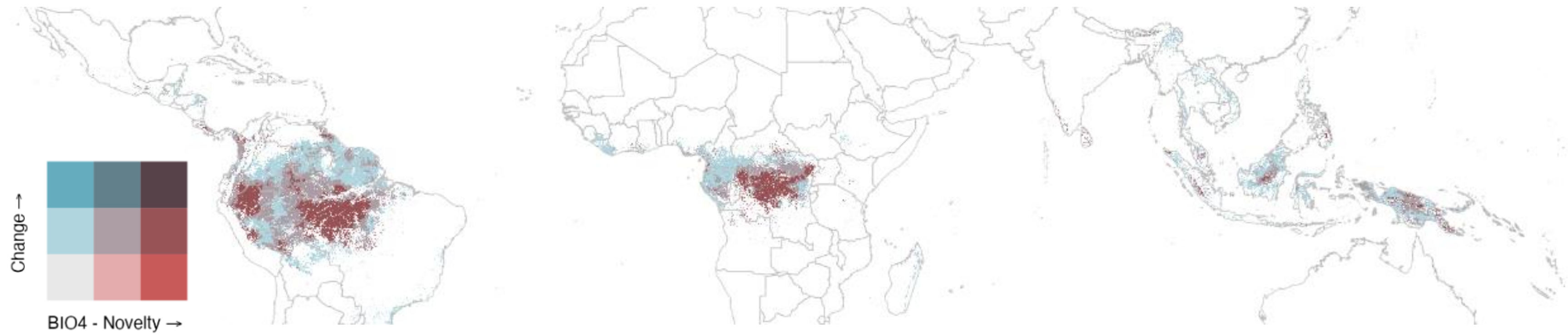


**Fig. S4-4: Spatial relationship between the overall change (°C) and the recent novelty of temperature seasonality.** Change is defined as the difference between the mean of the temperature variable for 1990-2004 and the mean for 2005-2019.


**Fig. S4-5: Spatial relationship between the overall change (°C) and the recent novelty of maximum temperature of the warmest month.** Change is defined as the difference between the mean of the temperature variable for 1990-2004 and the mean for 2005-2019.

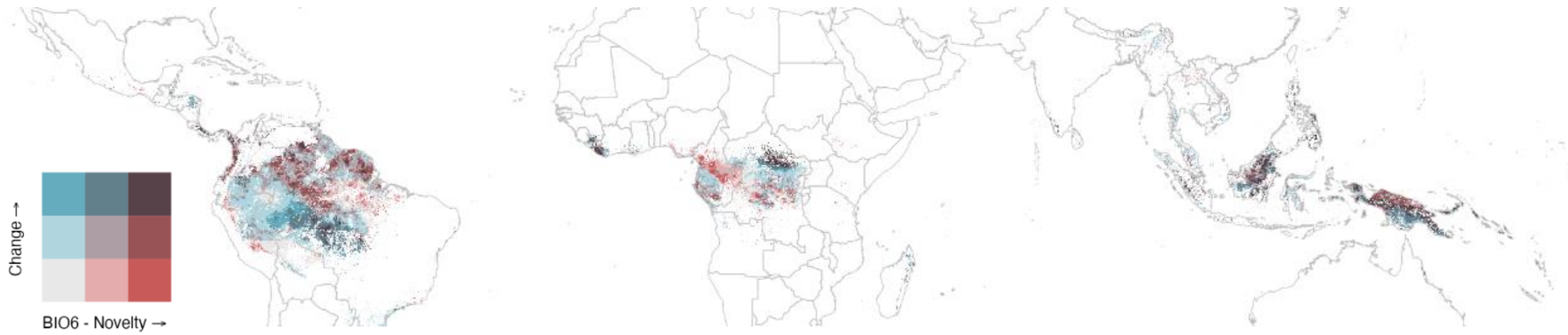


**Fig. S4-6: Spatial relationship between the overall change (°C) and the recent novelty of minimum temperature of the coldest month.** Change is defined as the difference between the mean of the temperature variable for 1990-2004 and the mean for 2005-2019.


**Fig. S4-7: Spatial relationship between the overall change (°C) and the recent novelty of annual temperature range.** Change is defined as the difference between the mean of the temperature variable for 1990-2004 and the mean for 2005-2019.

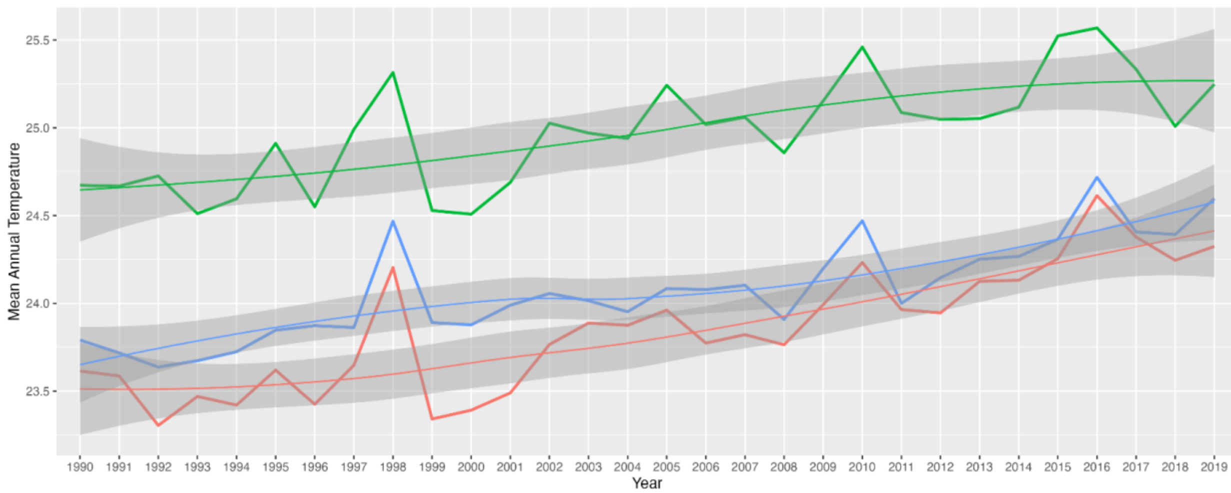


**Fig. S5-1: Time series plots of below-canopy mean annual temperatures from 1990 to 2019, averaged across all grid cells in each continental group.** Overall long-term change shown as a trend line for Central & South America (green), Africa (red), and South-East Asia & Australia (blue) respectively: 0.41, 0.50, 0.37. The grey shaded area represents a 95% confidence interval.

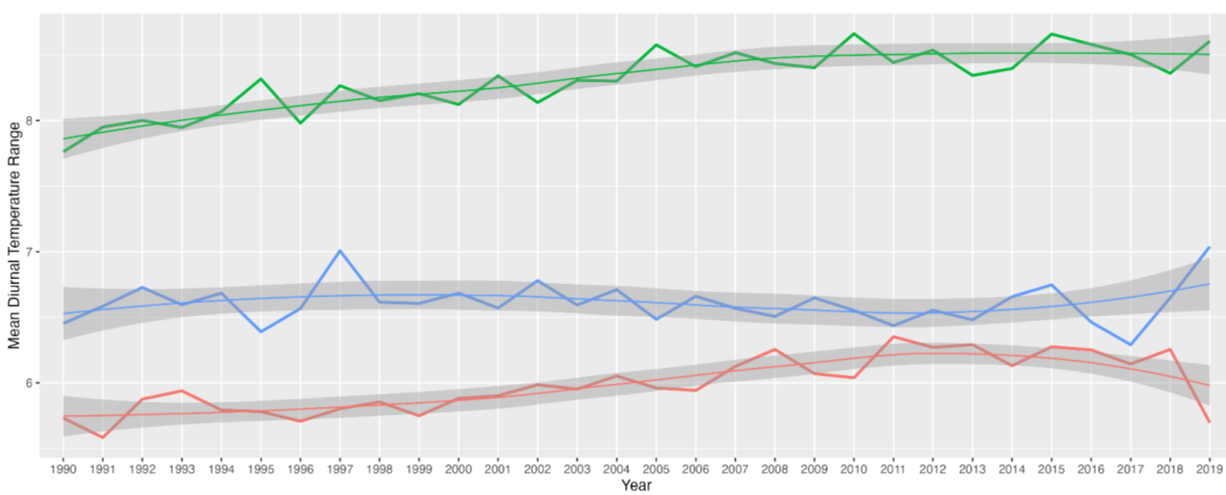


**Fig. S5-2: Time series plots of below-canopy mean diurnal temperature ranges from 1990 to 2019, averaged across all grid cells in each continental group.** Overall long-term change shown as a trend line for Central & South America (green, n = 185,883), Africa (red, n = 67,799), and South-East Asia & Australia (blue, n = 64,127) respectively: 0.37, 0.30, -0.06. The grey shaded area represents a 95% confidence interval.

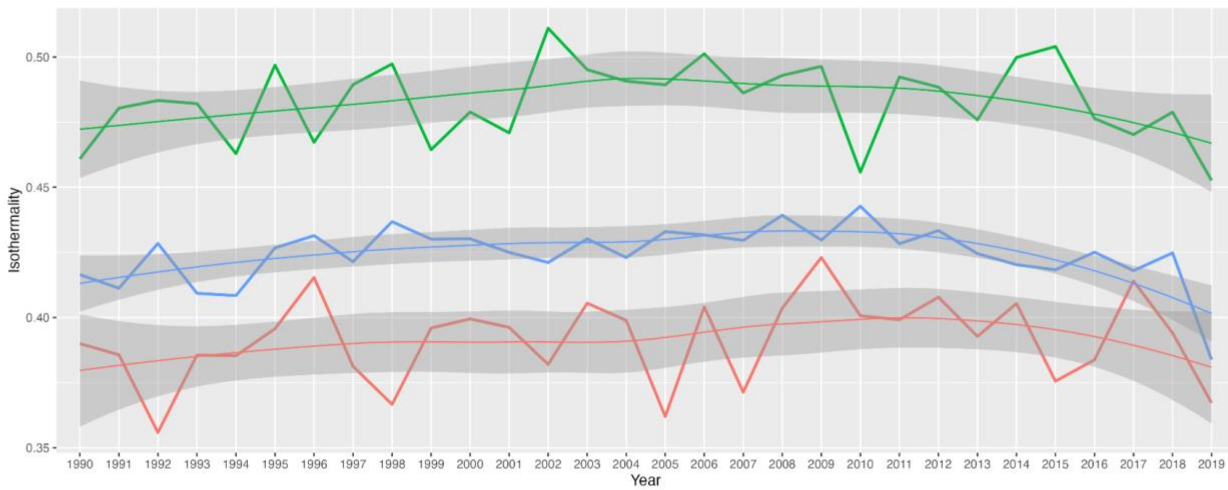


**Fig. S5-3: Time series plots of below-canopy temperature isothermality from 1990 to 2019, averaged across all grid cells in each continental group.** Overall long-term change shown as a trend line for Central & South America (green, n = 185,883), Africa (red, n = 67,799), and South-East Asia & Australia (blue, n = 64,127) respectively: 0.002, 0.004, 0.002. The grey shaded area represents a 95% confidence interval.

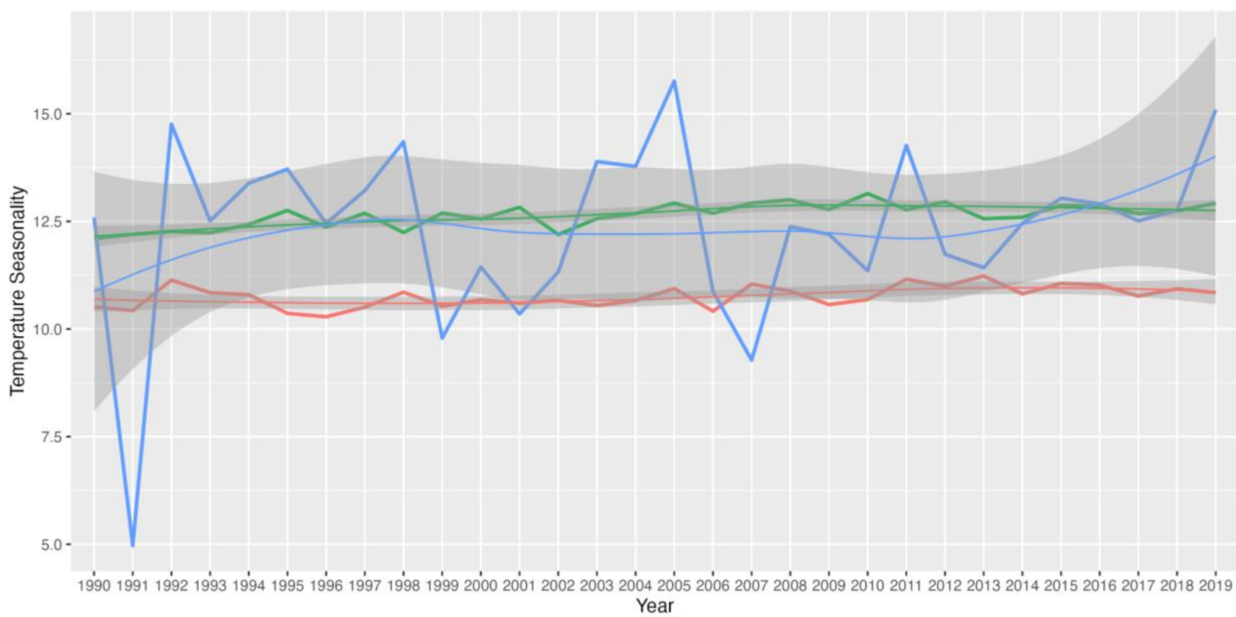


**Fig. S5-4: Time series plots of below-canopy temperature seasonality from 1990 to 2019, averaged across all grid cells in each continental group.** Overall long-term change shown as a trend line for Central & South America (green, n = 185,883), Africa (red, n = 67,799), and South-East Asia & Australia (blue, n = 64,127) respectively: 0.37, 0.26, 0.37. The grey shaded area represents a 95% confidence interval.

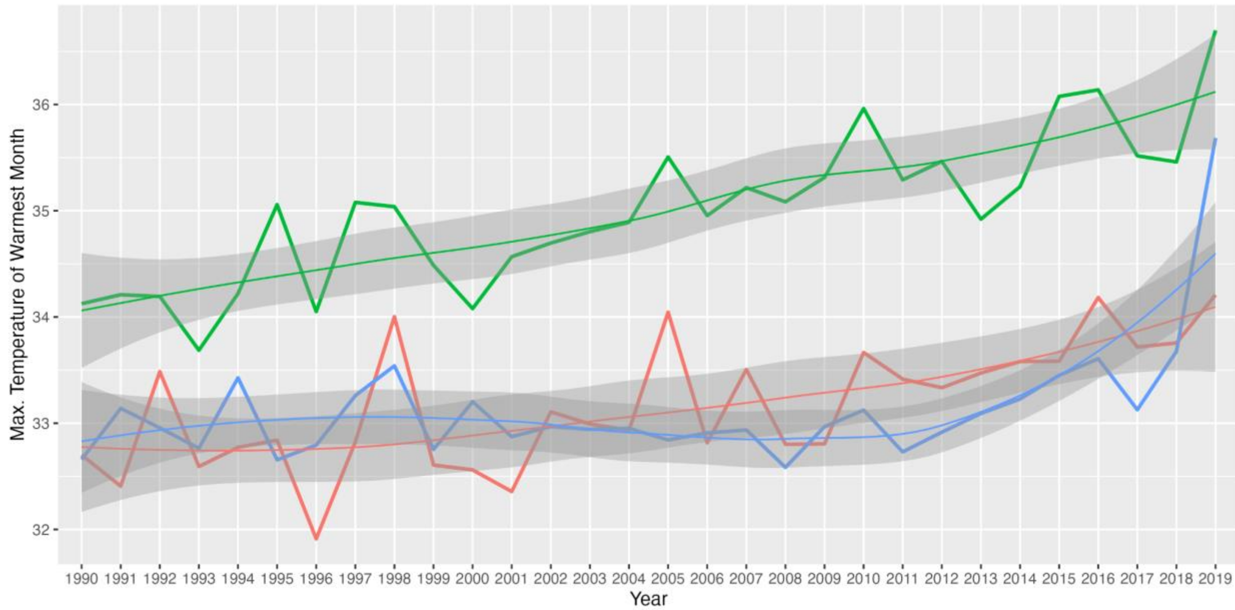


**Fig. S5-5: Time series plots of below-canopy maximum temperature of the warmest month from 1990 to 2019, averaged across all grid cells in each continental group.** Overall long-term change shown as a trend line for Central & South America (green, n = 185,883), Africa (red, n = 67,799), and South-East Asia & Australia (blue, n = 64,127) respectively: 1.04, 0.72, 0.27. The grey shaded area represents a 95% confidence interval.

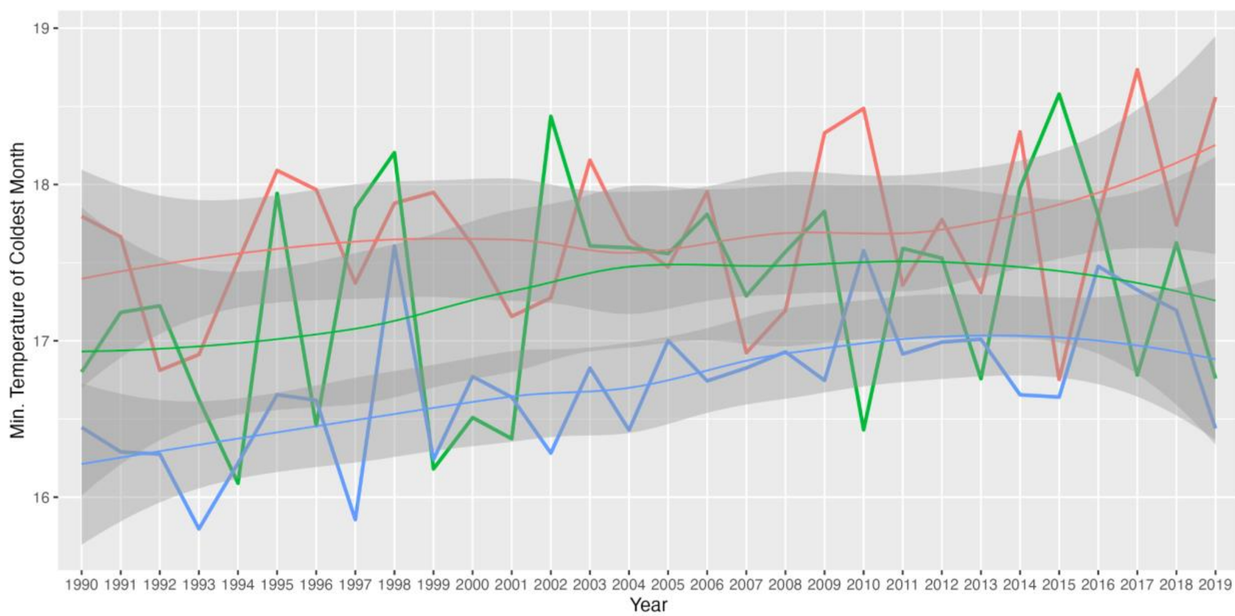


**Fig. S5-6: Time series plots of below-canopy minimum temperature of the coldest month from 1990 to 2019, averaged across all grid cells in each continental group.** Overall long-term change shown as a trend line for Central & South America (green, n = 185,883), Africa (red, n = 67,799), and South-East Asia & Australia (blue, n = 64,127) respectively: 0.32, 0.19, 0.50. The grey shaded area represents a 95% confidence interval.

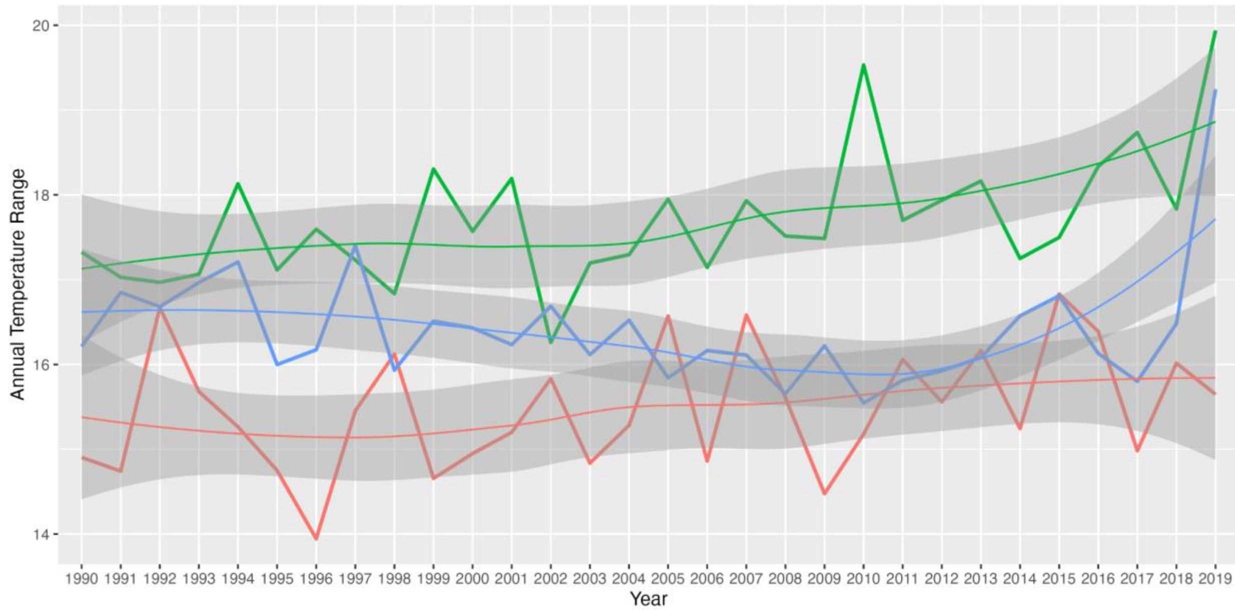


**Fig. S5-7: Time series plots of below-canopy annual temperature range from 1990 to 2019, averaged across all grid cells in each continental group.** Overall long-term change shown as a trend line for Central & South America (green, *n = 185,883*), Africa (red, *n = 67,799*), and South-East Asia & Australia (blue, *n = 64,127*) respectively: 0.72, 0.52, -0.24. The grey shaded area represents a 95% confidence interval.

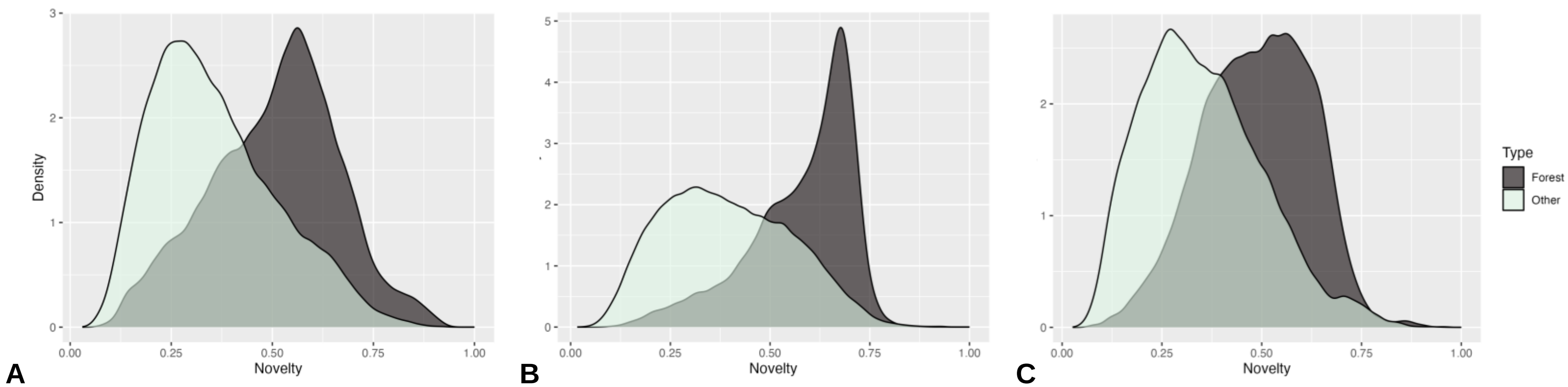


**Fig. S6-1: Frequency distribution for the novelty of mean annual temperature within tropical forest (*n = 374,197*) and outside of tropical forest (*n = 1,200,813*).** For (A) Central & South America (29.94°S–30.05°N, 109.98°W–30.04°E), (B) Africa (29.74°S–19.99°S, 19.79°E–57.74°E), and (C) Asia & Australia (23.49°S–69.99°N, 28.04°E–178.98°E), values outside of tropical forest are defined as grid cells which are neither undisturbed or degraded forest in 2019. Values inside of tropical forest are defined as undisturbed or degraded forest in 2019.

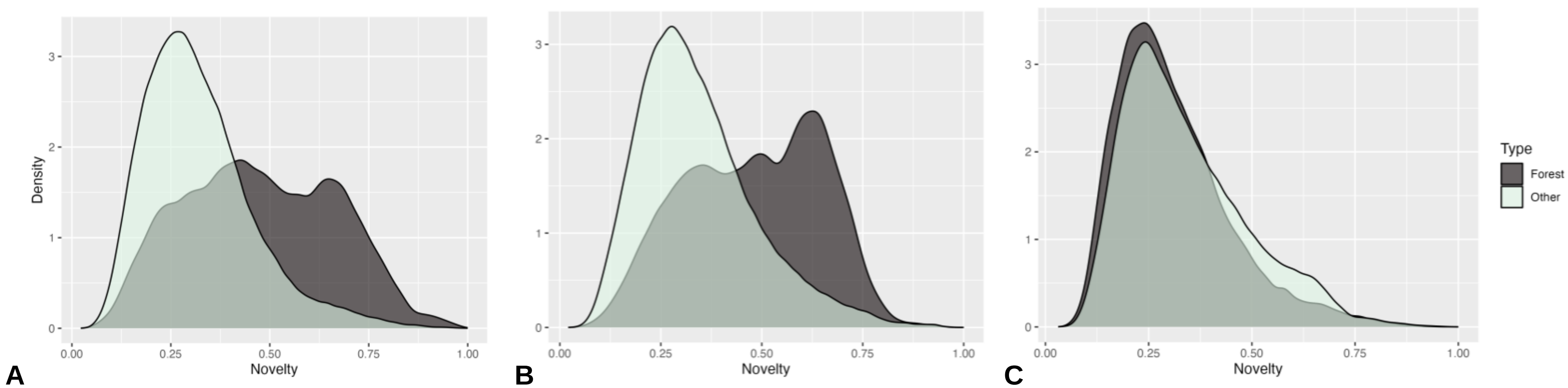


**Fig. S6-2: Frequency distribution for the novelty of mean diurnal temperature range within tropical forest (*n = 374,197*) and outside of tropical forest (*n = 1,200,813*).** For (A) Central & South America (29.94°S–30.05°N, 109.98°W–30.04°E), (B) Africa (29.74°S–19.99°S, 19.79°E–57.74°E), and (C) Asia & Australia (23.49°S–69.99°N, 28.04°E–178.98°E), values outside of tropical forest are defined as grid cells which are neither undisturbed or degraded forest in 2019. Values inside of tropical forest are defined as undisturbed or degraded forest in 2019.

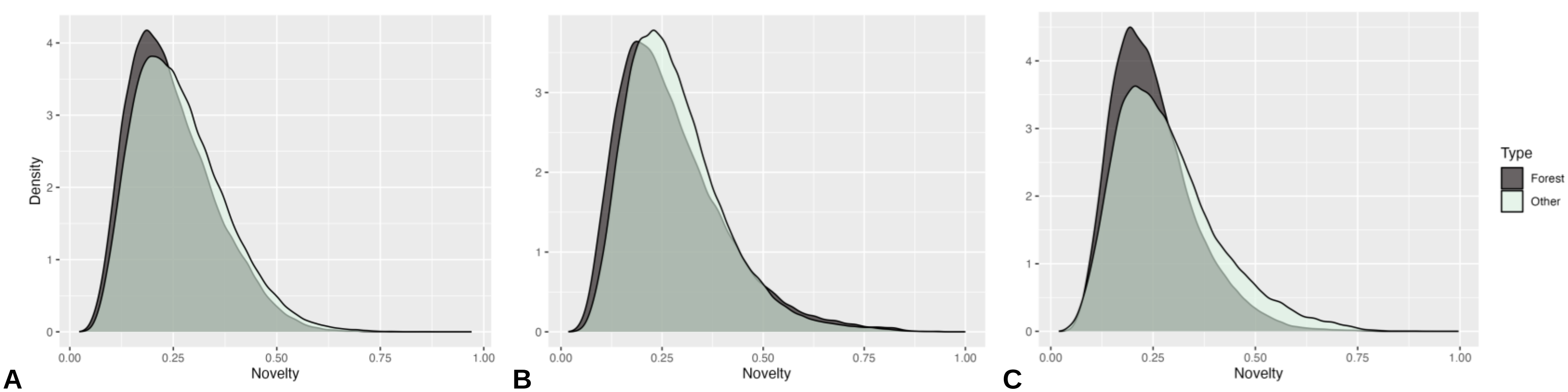


**Fig. S6-3: Frequency distribution for the novelty of isothermality within tropical forest (*n = 374,197*) and outside of tropical forest (*n = 1,200,813*).** For (A) Central & South America (29.94°S–30.05°N, 109.98°W–30.04°E), (B) Africa (29.74°S–19.99°S, 19.79°E–57.74°E), and (C) Asia & Australia (23.49°S–69.99°N, 28.04°E–178.98°E), values outside of tropical forest are defined as grid cells which are neither undisturbed or degraded forest in 2019. Values inside of tropical forest are defined as undisturbed or degraded forest in 2019.

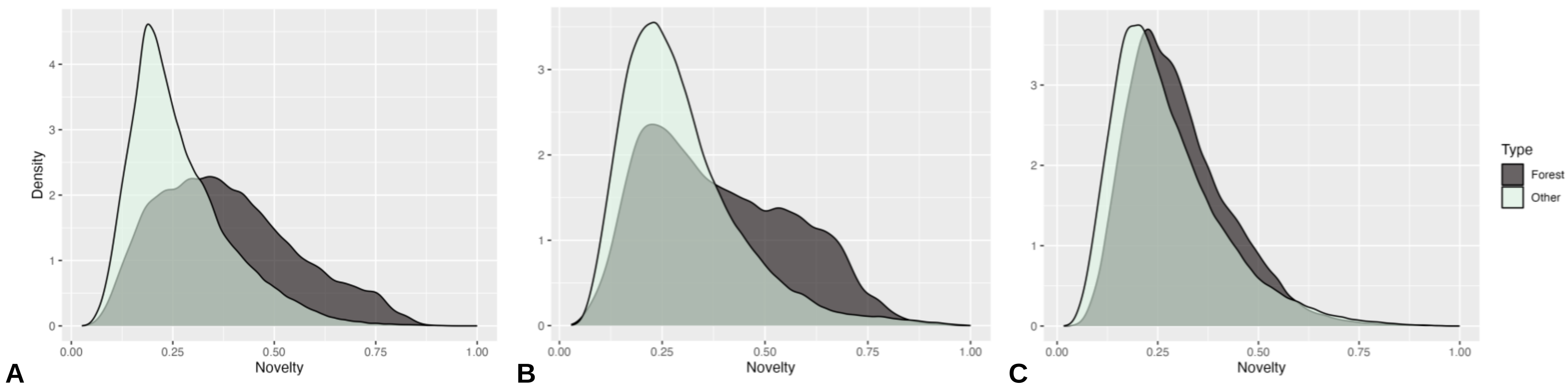


**Fig. S6-4: Frequency distribution for the novelty of temperature seasonality within tropical forest (*n = 374,197*) and outside of tropical forest (*n = 1,200,813*).** For (A) Central & South America (29.94°S–30.05°N, 109.98°W–30.04°E), (B) Africa (29.74°S–19.99°S, 19.79°E–57.74°E), and (C) Asia & Australia (23.49°S–69.99°N, 28.04°E–178.98°E), values outside of tropical forest are defined as grid cells which are neither undisturbed or degraded forest in 2019. Values inside of tropical forest are defined as undisturbed or degraded forest in 2019.

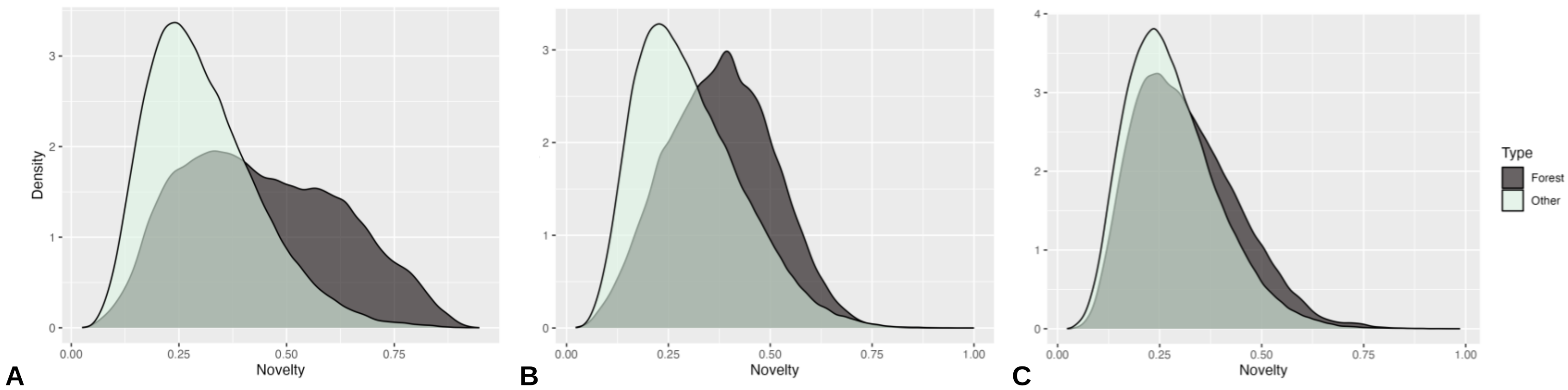


**Fig. S6-5: Frequency distribution for the novelty of maximum temperature of the warmest month within tropical forest (*n = 374,197*) and outside of tropical forest (*n = 1,200,813*).** For (A) Central & South America (29.94°S–30.05°N, 109.98°W–30.04°E), (B) Africa (29.74°S–19.99°S, 19.79°E–57.74°E), and (C) Asia & Australia (23.49°S–69.99°N, 28.04°E–178.98°E), values outside of tropical forest are defined as grid cells which are neither undisturbed or degraded forest in 2019. Values inside of tropical forest are defined as undisturbed or degraded forest in 2019.

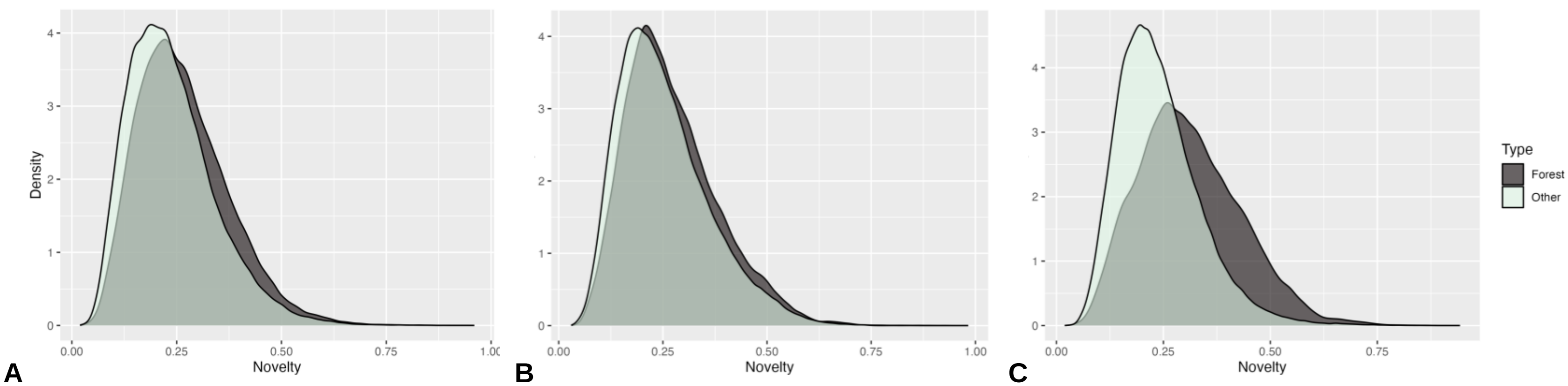


**Fig. S6-6: Frequency distribution for the novelty of minimum temperature of the coldest month within tropical forest (*n = 374,197*) and outside of tropical forest (*n = 1,200,813*).** For (A) Central & South America (29.94°S–30.05°N, 109.98°W–30.04°E), (B) Africa (29.74°S–19.99°S, 19.79°E–57.74°E), and (C) Asia & Australia (23.49°S–69.99°N, 28.04°E–178.98°E), values outside of tropical forest are defined as grid cells which are neither undisturbed or degraded forest in 2019. Values inside of tropical forest are defined as undisturbed or degraded forest in 2019.

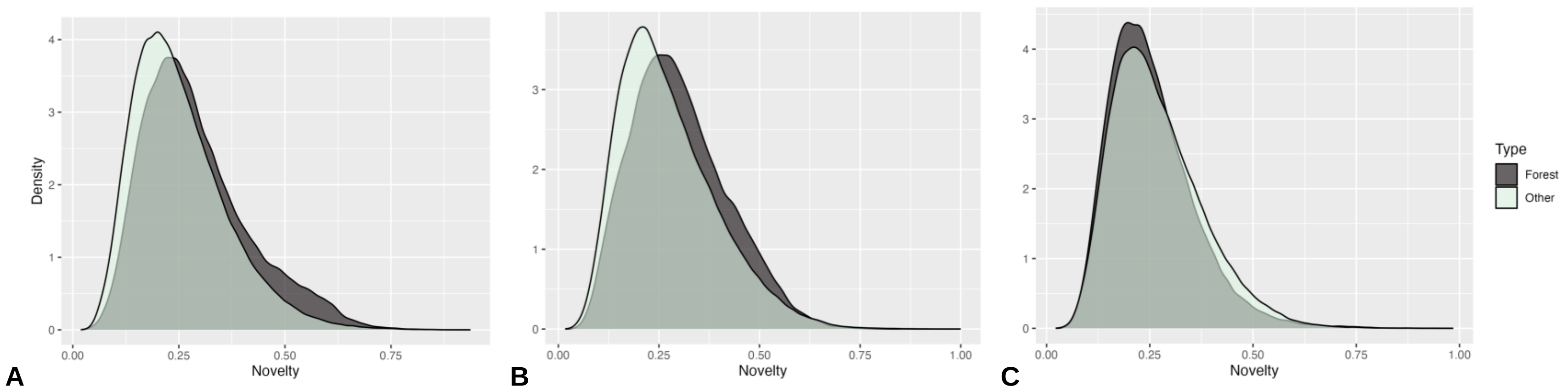


**Fig. S6-7: Frequency distribution for the novelty of annual temperature range within tropical forest (*n = 374,197*) and outside of tropical forest (*n = 1,200,813*).** For (A) Central & South America (29.94°S–30.05°N, 109.98°W–30.04°E), (B) Africa (29.74°S–19.99°S, 19.79°E–57.74°E), and (C) Asia & Australia (23.49°S–69.99°N, 28.04°E–178.98°E), values outside of tropical forest are defined as grid cells which are neither undisturbed or degraded forest in 2019. Values inside of tropical forest are defined as undisturbed or degraded forest in 2019.

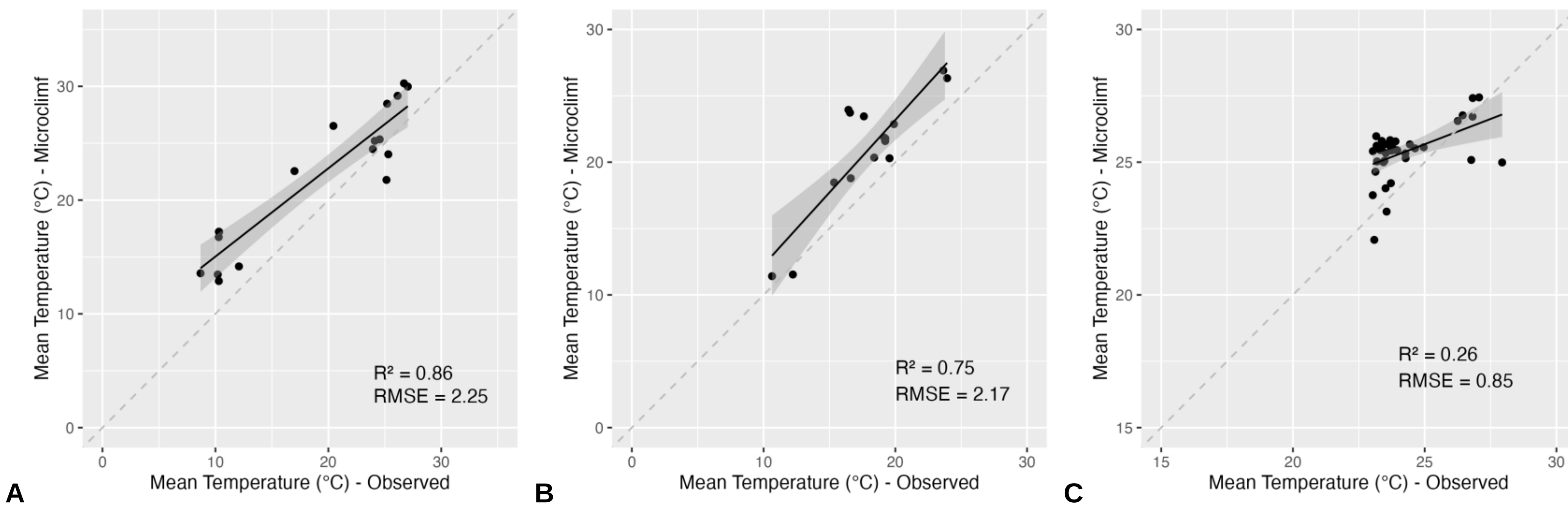


**Fig. S7-1: Relationship between mean temperatures modeled using *microclimf* and mean temperatures recorded by in-situ temperature loggers.** These results pertain to temperatures beneath tropical forest canopies across (A) South America, (B) Africa and (C) South-East Asia. The grey shaded areas represent 95% confidence intervals.

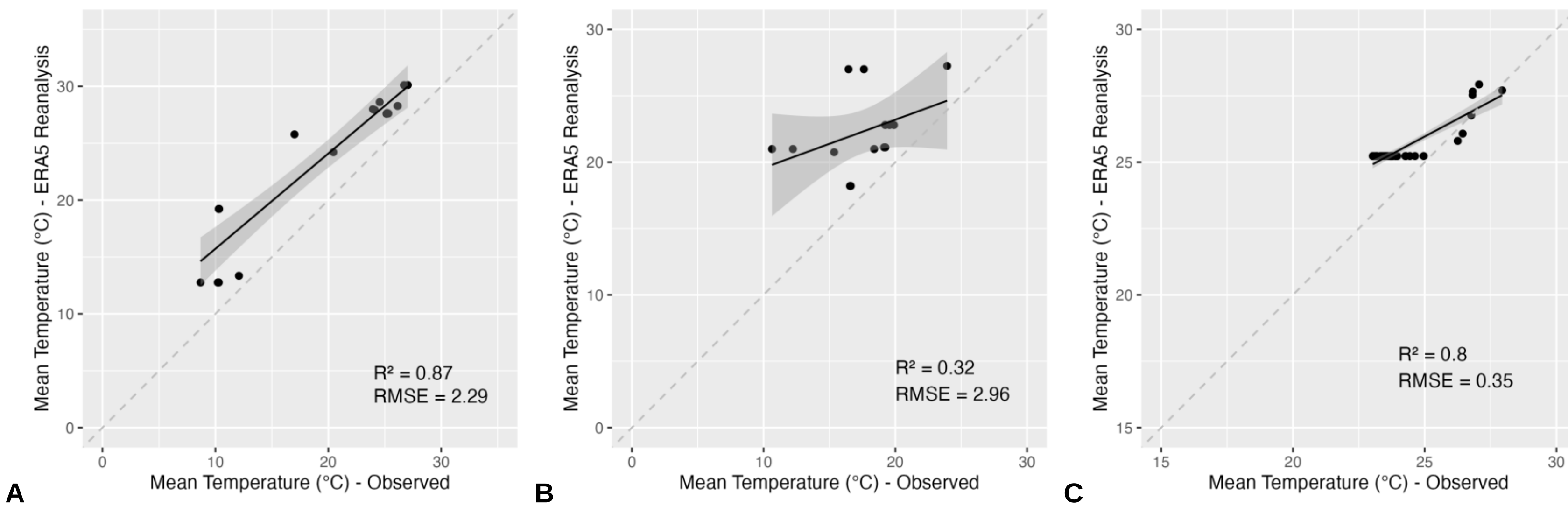


**Fig. S7-2: Relationship between mean temperatures modeled using the ERA5 reanalysis dataset and mean temperatures recorded by in-situ temperature loggers.** These results pertain to temperatures beneath tropical forest canopies across (A) South America, (B) Africa and (C) South-East Asia. The grey shaded areas represent 95% confidence intervals.

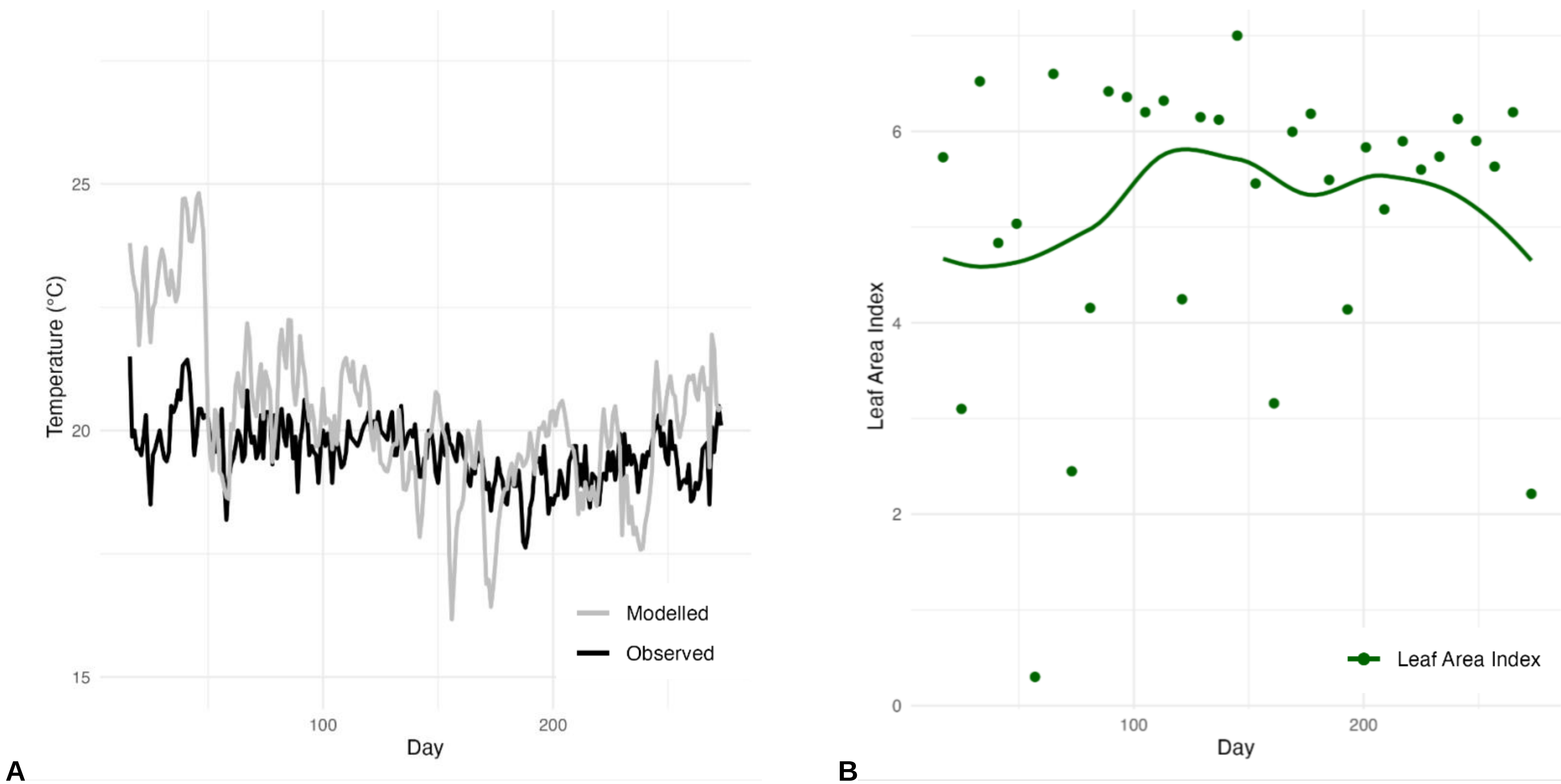


**Fig. S8: Time series plots relating daily variation leaf area index and mean temperatures.** (A) Mean daily temperatures for 2018 recorded by a temperature logger located in Uganda (longitude: 30.387; latitude: 0.451) and modeled as below-canopy mean daily temperatures (as per the methods described for validation). (B) Leaf area index values, derived from remote sensing methods (Myneni et al., 2015), corresponding to the logger's location. Leaf area index values were used to drive the mechanistic microclimate model.

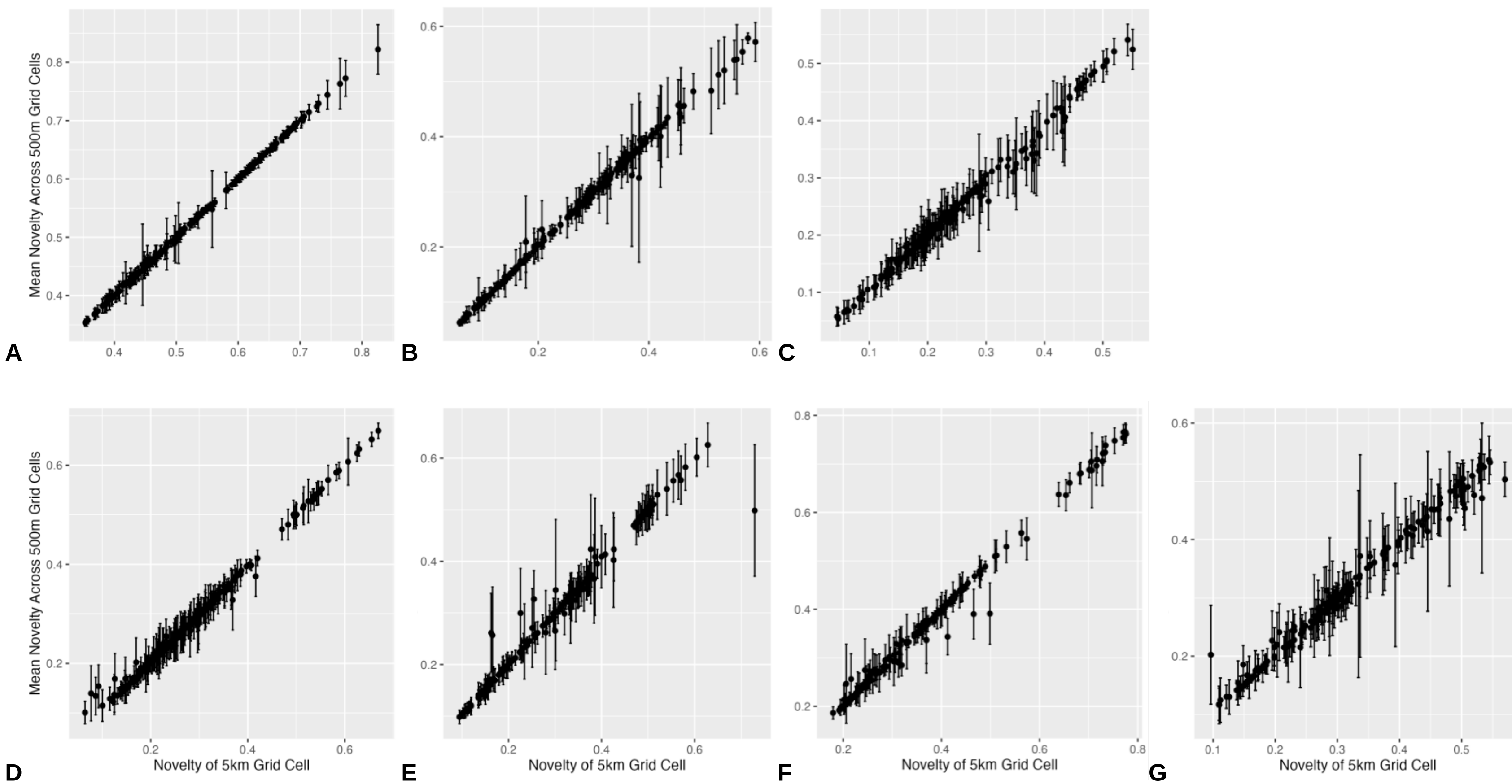


**Fig. S9: Comparisons of fine-scale variation in novelty with coarser novelty scores.** Plots of the mean novelty of (A) mean annual temperature, (B) mean diurnal temperature range, (C) isothermality, (D) temperature seasonality, (E) maximum temperature of the warmest month, (F) minimum temperature of the coldest month, (G) annual temperature range when modeled at a 500 m gridded resolution compared with novelty values of the same variable when modeled at a 5 km gridded resolution. A random subsample of 10 sites were used as the 5 km grid cells and these were then divided into 500 m grid cells.

**References.**

Batjes NH. Harmonised soil property values for broad-scale modelling (WISE30sec) with estimates of global soil carbon stocks. *Geoderma* **269**, 61-68 (2016). http://dx.doi.org:10.1016/j.geoderma.2016.01.034

Buchhorn, M.; Lesiv, M.; Tsendbazar, N.-E.; Herold, M.; Bertels, L.; Smets, B. Copernicus Global Land Cover Layers—Collection 2. *Remote Sens*., **12**, 1044 (2020). https://doi.org:10.3390/rs12061044

ESA. Land Cover CCI Product User Guide Version 2. Tech. Rep. (2017). Available at: maps.elie.ucl.ac.be/CCI/viewer/download/ESACCI-LC-Ph2-PUGv2_2.0.pdf

Fujisada, H., Bailey, G.B., Kelly, G.G., Hara, S., Abrams, M.J. ASTER DEM performance. IEEE *Transactions on Geoscience and Remote Sensing* **43**, 2707-2714 (2005). https://doi.org:10.1109/TGRS.2005.847924

Hersbach, H. et al. The ERA5 global reanalysis. *Quarterly Journal of the Royal Meteorological Society* **146**, 1999-2049 (2020). https://doi.org:10.1002/qj.3803

Myneni, R.B., Hoffman, S., Knyazikhin, Y., Privette, J.L., Glassy, J., Tian, Y., Wang, Y., Song, X., Zhang, Y., Smith, G.R., Lotsch, A., Friedl, M., Morisette, J.T., Votava, P., Nemani, R.R., Running, S.W. Global products of vegetation leaf area and fraction absorbed PAR from year one of MODIS data. *Remote Sensing of Environment* **83**, 214-231 (2002). https://doi.org:10.1016/S0034-4257(02)00074-3.

Potapov, P., Li, X., Hernandez-Serna, A., Tyukavina, A., Hansen, M.C., Kommareddy, A., Pickens, A., Turubanova, S., Tang, H., Silva, C.E., Armston, J., Dubayah, R., Blair, J.B., Hofton, M. Mapping global forest canopy height through integration of GEDI and Landsat data. *Remote Sensing of Environment* **253**, 112165 (2021). https://doi.org:10.1016/j.rse.2020.112165.

Simard, M., Pinto, N., Fisher, J.B., Baccini, A. Mapping forest canopy height globally with spaceborne lidar. Journal of Geophysical Research: *Biogeosciences* **116** (2011). https://doi.org:10.1029/2011JG001708.